Aust. Met. Mag. 39 (1991) 167–180

A numerical scheme for tracking cyclone centres from digital data Part II: application to January and July general circulation model simulations

Ross J. Murray and Ian Simmonds
Department of Meteorology, University of Melbourne, Australia
(Manuscript received November 1990; revised March 1991)

An objective scheme (described in Part I) has been used to study the distribution and movement of southern hemisphere extratropical cyclones generated by a general circulation model for January and July. The model cyclones reproduced a number of the important features of cyclone behaviour reported from earlier observational studies. Systems moved in the expected east-southeast direction, with maximum speeds in mid-latitudes. The circumpolar trough and the major Antarctic embayments were found to be regions of maximum cyclone density and of net dissipation. Contrary to earlier findings they were also found to be regions of active local cyclogenesis. The model results appear to correspond rather more closely to the distribution revealed from recent ECMWF analyses than from earlier studies.

Introduction

We have reached the point at which a number of global models are providing good simulations of the mean state of the atmosphere and are becoming increasingly relied upon for investigating the effects of changes to its forcing. Evidence suggests that current general circulation models are able to capture the observed levels of variability (e.g. Simmonds and Dix 1989; Simmonds et al. 1990) but it has not been clear whether individual lows and frontal systems are well modelled. This is of particular importance in the mid-latitudes of the southern hemisphere (SH), where virtually all of the atmospheric poleward heat flux is effected by the transient eddies (Oort and Peixóto 1983).

Until recently, synoptic climatologies for the SH have all been performed by manual techniques and none have been carried out for model results. However, two authors have recently used objective methods to study cyclone distributions. Lambert (1988) used an automated cyclone finding program to calculate and compare observed and simulated area-normalised cyclone densities averaged over five northern hemisphere (NH) and SH winters. Le Treut and Kalnay (1990), using a scheme to find and track cyclone centres, compared observed and simulated frequencies of NH and SH cyclone occurrence, cyclogenesis and cyclolysis for the two 50-day Special Observing Periods of the First GARP Global Experiment (1979).

In this paper we present the results of a study of the behaviour of January and July SH extratropical cyclones generated by the Melbourne University general circulation model (GCM) (Simmonds 1985; Simmonds et al. 1988; Simmonds and Dix 1989). An automated scheme, described in Part I (Murray and Simmonds 1991) has been used to locate and track depressions from numerical mean sea level (MSL) pressure analyses. The methods used are somewhat more complex than those used by the schemes referred to above. A summary of the principal features of the scheme is given in the next section.

We have compared our results with a number of observational studies of SH cyclones dating from the 1960s. The early compilations of Karelsky (1961,1963) (recently updated by Leighton and

Corresponding author address: Dr I. Simmonds, Department of Meteorology, University of Melbourne, Parkville, Victoria 3052, Australia.

Deslandes (1989)) give cyclone and anticyclone statistics for the Australian region based upon long series of synoptic data. His latter paper includes the only maps of central pressures available. The first definitive synoptic climatology for the entire SH was published by Taljaard (1967), who plotted tracks of cyclones and anticyclones over the SH and determined their patterns of movement and distribution in the four seasons, using analyses prepared during the IGY (1957–58). His work is complemented by the frequencies of surface fronts in summer and winter during the earlier part of the IGY by van Loon (1965). Following a subsequent data gathering effort, Neal (1972) plotted tracks and cyclogeneses and gave the regional distributions of anticyclones, cyclones and cyclogenesis for the two single months of the GARP Basic Data Set Analysis Project (November 1969 and June 1970).

In two studies cyclone movements were derived from the analysis of cloud imagery. Streten and Troup (1973) found the geographical variation of vortex frequencies and speeds according to state of development for the summer and intermediate seasons over the period November 1966 to March 1969. Regions of cyclogenesis were associated with high frequencies of early development vortices (types W, A and B in the classification of Troup and Streten (1972)) and cyclolysis with those of dissipating vortices (type D). Carleton (1979) followed this up with an investigation of winter cyclonic activity during the five SH winters 1973–77 using infrared imagery.

Le Marshall and Kelly (1981), in their account of the SH climatology derived from World Meteorological Centre analyses, showed the regionally and zonally averaged anticyclone and cyclone densities for January and July 1973–77. Kep (1984) plotted and tracked cyclones from the positions of lows marked on operational analyses for each month during the ten-year period 1972–81 and prepared tables of frequencies of cyclones and cyclogenesis.

A variety of data periods and analysis methods have been used in the various works cited above. Summer and winter have been associated with the single months of January and July or with periods of several months. Most workers have given frequencies as areal densities, but Kep has measured cyclone occurrence in numbers of tracks crossing 10° meridian segments at 10° longitude intervals. Taljaard (1967) defined a low as being a centre with a closed contour at a contour interval of 2.5 hPa, Kep (1984) used the centres marked on operational charts, while Streten and Troup (1973) and Carleton (1979) identified cyclones from vortex signatures. In the GCM study described here, both open and closed cyclonic features have been analysed, subject to a minimum cyclonic curvature in the pressure surface. This diversity should be allowed for in making comparisons.

Application of the scheme

Finding and tracking the lows

The GCM data to which the scheme was applied uses spherical harmonic basis functions rhomboidally truncated at wave number 21, with 9 levels in the vertical. It is forced by 'perpetual' diurnally-averaged January or July insolation with specified albedo, specified concentrations of carbon dioxide and ozone, and prescribed seasonal sea-surface temperatures and snow, sea-ice and cloud cover. The GCM incorporates moist convective adjustment and a surface layer based on Monin-Obukhov similarity theory. The model is run for an initial 60 days to allow the atmosphere to stabilise and then for a further 600 days. Surface pressures (p_s) are reduced to MSL by downward integration of the hydrostatic equation from lowest model sigma level ($p=0.991p_s$), assuming a lapse rate of 6.5°C/km.

The daily MSL pressures produced by the model for days 61 to 660 were interpolated onto a 61×61 SH polar stereographic (PS) grid, which has a resolution of 3.8 deg. lat. at the South Pole. This grid was used in all stages of the scheme.

In the first stage of the scheme the centres of lows were positioned using an iterative differential routine, with pressures and pressure derivatives being defined by bicubic spline interpolation. Two types of cyclonic centre were analysed. The centres of closed depressions were located by minimising the pressure. Open depressions (cyclonic disturbances with no closed isobars) were identified with points of inflexion on the interpolated pressure surface and were located by minimising the absolute value of the pressure gradient. To exclude heat lows and other insignificant cyclonic features unlikely to be associated with migratory storms, a criterion was applied (hereinafter known as the 'concavity test') which requires a minimum average value of $\nabla^2 p$ over a small area around the analysed centre. (The condition which was actually used stipulated that

$$\overline{\nabla^2 p} + 0.1\nabla^2 p \geq 0.5\text{hPa/(deg.lat.)}^2, \quad \ldots 1$$

where the overbar designates an average over the grid-points within a radius of 4 deg.lat.)

Cyclone paths were then tracked by a program which estimates the subsequent displacement and pressure change of each cyclone at each analysis time. The displacement is based on a weighting of the movement during the previous time interval and the climatological zonally averaged cyclone velocities, the pressure change on a weighting of previous tendency and persistence. Probabilities of association between the projected cyclones and those actually present at the following analysis time were computed on the basis of their differences in position and pressure. Matching was performed by determining the combination of associations having the greatest overall probability.

The numerical values of the chief parameters used for tracking the GCM cyclones are as follows:

w_M = 0.36
w_P = 0.30
k_{rp} = 1.4 hPa/deg. lat.
r_c = 12.5°
P_{open} = 0.6
P_{new} = 0.75

The meanings of these quantities and the methods used to locate and track the lows are as set out in Part I. The velocities originally used to aid the prediction of cyclone movements are not tabulated as these were subject to a process of optimisation, wherein the zonally averaged output velocity statistics were fed back into the tracking program and statistics were recalculated. This was repeated a few times until stable values were obtained.

Analysis of track statistics

The analysis program calculates zonal and regional averages of the frequency, velocity, central pressure and pressure tendency of cyclones, and the frequencies of cyclogenesis and cyclolysis from the accumulated track histories. Cyclone frequency has been reckoned both as a density and as a flux. Cyclone density refers to the average number of systems per unit area at any one time; cyclone track flux is used to denote the average number of systems passing within unit distance of any point per unit time. In the present study, flux has been reckoned as a vector quantity whose eastward and northward components represent the net number of eastward (northward) crossings per unit length of meridian (parallel) per unit time.

Inclusion of systems in the statistics was made conditional on the survival of a system for a minimum lifespan (i.e. the difference between the times at which it was first and last recorded) of 24 hours (2 analysis times), except in the case of cyclogenesis and cyclolysis for which a 72-hour minimum lifespan was stipulated. The zonal and regional statistics of cyclogenesis and cyclolysis were obtained from the counts of the first and last recorded positions of each system. For calculating the other quantities, the position coordinates and central pressures of each system, and their tendencies, were interpolated by cubic splines at 1/5-day intervals and statistics were aggregated from all sampled (recorded and interpolated) positions. Regional distributions were compiled on the PS grid with the application of a smoothing procedure. Zonal means were computed from summations over 5° latitude intervals and were not smoothed. Summations of cyclogenesis and cyclolysis were normalised for area and time; those of cyclone density and net flux were normalised for area and number of sampling periods. The area for each grid-point was taken as the square of the map factor (3.82 deg. lat. $\times \cos^{2}[1/2(\phi_{pole}-\phi)]$).

Smoothing of the regional statistics was carried out as follows. The average values of system properties (velocity, pressure and pressure tendency) were obtained by contributing a weighted fraction of the value, q_k, of the quanity, q, at each sampled position, k, to the total for each grid-point (i, j) within the radius $r_{ijk}<r_{s1}$. The weighting factors were of the form,

$$w_{ijk} = w(r_{ijk}) = \frac{r_{s1}^2 - r_{ijk}^2}{r_{s1}^2 + r_{ijk}^2(r_{s1}^2/r_{s2}^2 - 1)}, \quad (r_{ijk} < r_{s1}), \qquad \ldots 2$$

where r_{ijk} is the distance between the grid-point (i, j) and the sampled position, k, and $w(r)$ was a function chosen to decrease monotonically from $1(r=0)$ to 0 $(r \geqslant r_{s1})$, with most of the fall-off occurring within a radius r_{s2}. The sum of the weighted values of the appropriate quantity, q_{ij}, for each grid-point, taken over the entire run, was divided by the sum of the weights for the grid-point, i.e.

$$\bar{q}_{ij} = \frac{\sum_k q_k w_{ijk}}{\sum_k w_{ijk}}. \qquad \ldots 3$$

Values of $r_{s1}=10$ deg. lat. and $r_{s2}=2.5$ deg. lat. were selected to ensure continuity of the analysis in poorly represented locations and give an accurate, but not too noisy, plot.

In the case of frequency distributions the same weighting function was used but the sum of the weighted counts distributed for each sampled position was normalised to unity. A smaller pass radius was used ($r_{s1}=5$ deg. lat.) since continuity was not required. Cyclone density was reckoned,

$$\bar{f}_{ij} = N\sum_k \left(\frac{w_{ijk}}{\sum_{i'j'} w_{i'j'k}}\right), \qquad \ldots 4$$

where the summation in the denominator effectively extends over the grid-points within a radius r_c of each sampled position, k, and N is a normalisation factor for area and sampling period. Frequencies of cyclogeneses and cyclolyses were similarly calculated, only the starting and finishing positions, respectively, being counted. Net flux was found as for cyclone density except that the weight apportioned to each grid-point was multiplied by the sampled velocity, i.e.,

$$\bar{\mathbf{F}}_{ij} = N\sum_k \left(\frac{w_{ijk}\mathbf{v}_k}{\sum_{i'j'} w_{i'j'k}}\right). \qquad \ldots 5$$

The zonally averaged net flux was taken to be given, with sufficient accuracy, by the product of the zonally averaged velocity and cyclone density.

Regional averages

Figure 1 shows the storm tracks for January and July and gives an impression of their alignment, density and variability. To reduce the clutter, only lows from the second half of each simulation (days 361–660) and lasting four or more daily positions (72 hours lifespan) are shown. The statistics which follow have, however, been compiled for all systems having a lifespan of at least 24 hours, unless otherwise stated. Variation between the patterns of tracks plotted for the first and second 300 days of each model run was imperceptible, which seems to indicate that the 600-day integration period constitutes a representative time span for the construction of the GCM climatology.

Cyclone density

The distribution of cyclone occurrence is represented in contoured form in Fig. 2 as a spatial density. In both seasons one observes a high level of cyclonic activity over the high latitude oceans, the distribution being somewhat more closely confined towards the Antarctic coast in January than in July. Maximum densities occurred in the eastern sector at latitude 60°S, their location possibly being determined by the tighter meridional temperature gradients at these longitudes and by entrainment of tropical air in the south Atlantic, as discussed later. At higher latitudes one notes a tendency for depressions to congregate in the Ross and Weddell Seas and, in January, near Prydz Bay.

Fig. 1 Tracks of cyclones for (a) January and (b) July. (Only those for days 361–660 and lasting at least four daily positions are shown.)

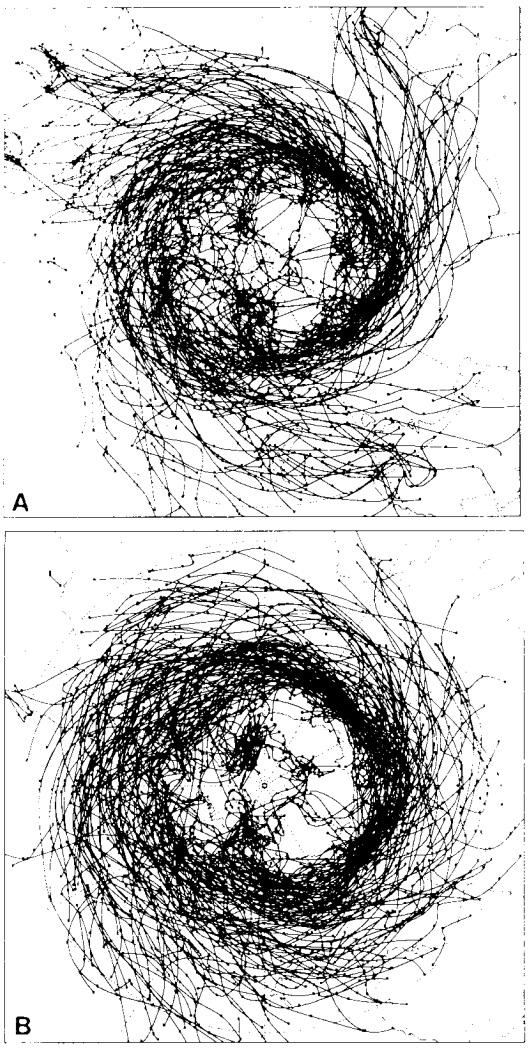

Fig. 2 Cyclone densities for (a) January and (b) July (contour interval 10^{-3} cyclones deg. lat.$^{-2}$).

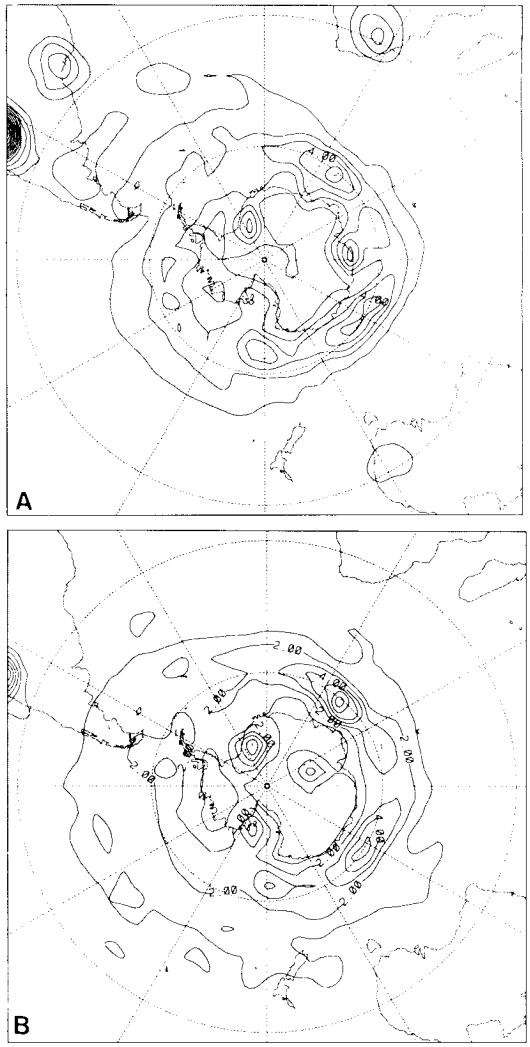

The high latitude distributions of cyclones are similar in form to those of Taljaard (1967) and Le Marshall and Kelly (1981), but peaked more strongly in the circumpolar trough around East Antarctica and extended further south than was found by abovementioned authors. Large numbers of cyclones were found in the Ross and Weddell Sea areas. It is possible that the low frequencies reported in earlier studies may reflect the patchy gathering of data and the difficulty in observing cloud vortices in these regions. The GCM cyclone distribution shows much better agreement with the more recent observed densities of 1000 hPa geopotential lows calculated by Lambert (1988) from ECMWF analyses for the winters of 1980–84.

Many heat lows are evident in continental areas during summer, as might be expected. Taljaard found large numbers of depressions over northern Argentina in all seasons; however, the abnormal densities of lows over the Andes in our results for January and July are almost certainly connected with an unrealistic reduction of surface pressures to sea level.

Cyclone track flux

The vectors in Fig. 3 show the net flux of storm tracks for January and July. There is a fairly general east to east-southeast movement of systems throughout the mid-latitudes, with a maximum concentration of cyclone tracks at 60°S. The eastward component of the net flux is shown in contoured form in Fig. 4. This is the dominant component over the hemisphere, except at low latitudes and over Antarctica where there are some regions of negative (westward) flux. Not surprisingly, therefore, the pattern is similar to that of cyclone density, but it will be seen that vector averaging has all but eliminated any contribution from the random movements of spurious depressions over South America and of heat lows over the subtropical continents, indicating that the shallower systems were not migratory in character.

A conspicuous feature of this plot and of the tracks in Fig. 1 is the strong channelling of cyclone paths along 60°S between 40°E and 120°E. The tracks of Kep (1984) are also more concentrated in the eastern sector but not nearly so sharply restricted in latitude. A similar discrepancy between simulated and observed behaviour was found by Le Treut and Kalnay (1990), who noticed a rather more tightly zonal alignment of tracks in a 20-day integration of the T-63 ECMWF forecast model than in the case of the ECMWF analyses for the same period (10–30 October 1979). The authors suggested that this might be related to an excessive zonalisation of the flow in the T-63 model which (like ours) does not incorporate gravity-wave drag.

A number of US authors have delineated characteristic cyclone and anticyclone tracks from ridges in frequency isopleths. The compilations of Klein (1957) and Whittaker and Horn (1982) show the 'principal tracks', or more correctly axes of high frequency, of systems in the NH for various months. The complexity of their patterns no doubt reflects the distribution of land and sea in that hemisphere. By comparison, the patterns of movement of cyclones in the SH appear to have much less structure.

The maps of Taljaard (1967) show well defined spiral arms of high cyclone frequency entering the circumpolar trough from the central South Pacific and the Gran Chaco of northern Argentina, particularly in winter. Similar axes were revealed in the frequencies of surface fronts for part of the same (IGY) period by van Loon (1965), in the distributions of early development vortices of

Fig. 3 Net flux vectors of cyclone tracks for (a) January and (b) July (1 grid space = 0.01 cyclones deg. lat.$^{-1}$ day^{-1}).

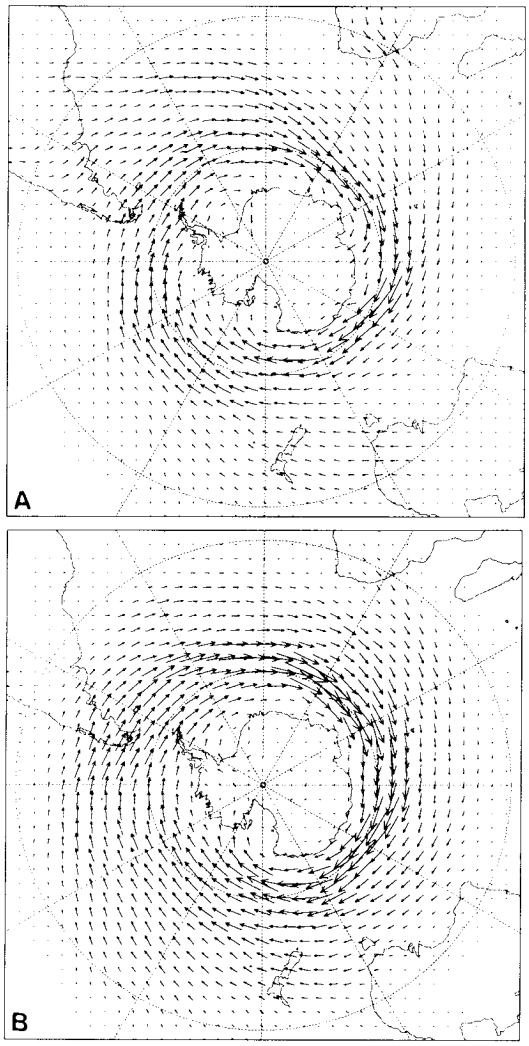

Fig. 4 Net eastward flux of cyclone tracks for (a) January and (b) July (contour interval 5×10^{-3} cyclones deg. lat.$^{-1}$ day^{-1}).

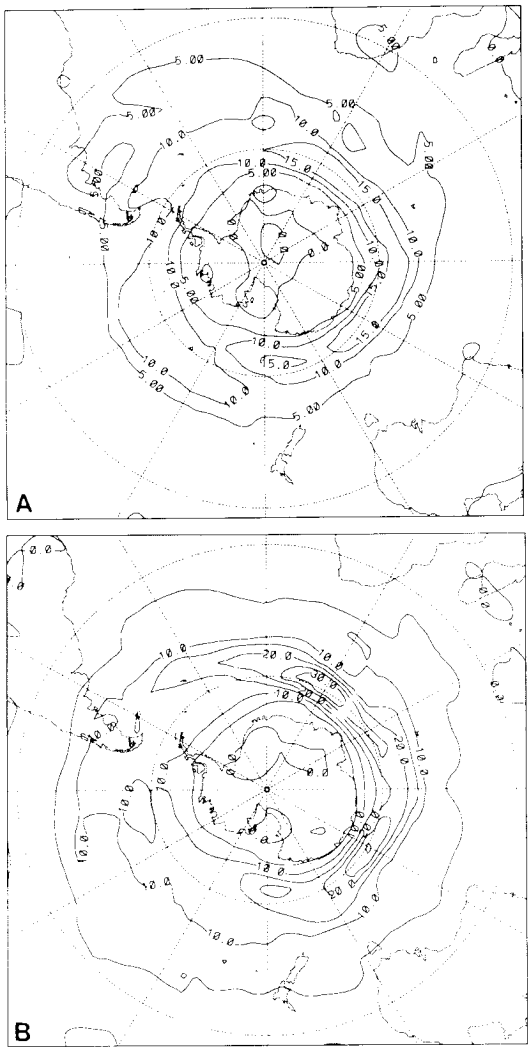

Streten and Troup (1973) and Carleton (1979), and in average brightness charts prepared from daily satellite cloud pictures for various seasons in 1969 by Yasunari (1977). By contrast, the averages of Le Marshall and Kelly (1981) and of Kep (1984) are rather more zonally symmetric and show little evidence of the features noted by Taljaard. The evidence appears, on balance, to support the belief that a weak development of spiral axes of high frequency over the western south Atlantic and central South Pacific Oceans is a persistent feature of the cyclone distribution.

Streten (1973) found that the axes of five-day averaged cloudiness were located close to the scale-separated 700 hPa long-wave troughs for the corresponding periods and suggested that the bands might represent the channels of energy flow into the mid-latitude westerlies. James and Anderson (1984) have shown that the trade wind easterlies, deflected by the Andes into the prevailing northwesterly winds over central South America, may constitute a source of low-level moisture which could be entrained in the mid-latitude westerly flow. This would encourage the growth of baroclinic waves over the south Atlantic, with downstream effects on the high frequency transient (cyclonic) activity over the Indian Ocean. A similar but less persistent mechanism was postulated over the central Pacific Ocean.

We can look for spiral arms in the plots of cyclone flux for the 600-day GCM simulations (Figs 2 and 4) and in the tracks in Fig. 1 (although it should be stressed that the alignment of frequency ridges is not necessarily the same as the average direction of movement of depressions). The development of these features was only rudimentary in July but more obvious in January. In the latter month there was a marked tendency for lows to form over continental areas, particularly South America, at around 20–30°S and track southeast across towards the westerly belt; this resulted in a considerable number of depressions passing over the western sides of the ocean basins at 30°S and almost none on the eastern sides. No indication of this phenomenon is evident in the tracks of Kep (1984).

Storm tracks south of 60°S, especially in January, tended to turn southwards and converge upon the Antarctic coast. The effect was most pronounced along the eastern shores of the major Antarctic embayments. Retrograde motion is quite common in respect of the tracks of individual systems; however, it is interesting to note in Fig. 3 a cyclonic curvature in the mean paths of cyclones, which is evident over the Ross and Weddell Seas.

Velocities

The mean eastward motion of cyclonic storms is shown in Fig. 5. A corresponding plot is not shown for the meridional component, but the directions of the velocity vectors are the same as for the net flux (Fig. 3). The distributions of average velocity components were fairly zonally symmetric, except for the undulations in the isotachs at lower latitudes which are suggestive of phase locking in the model, possibly associated with the specification of the model topography. Maximum eastward velocities were recorded in the 40–50°S latitude zone in both seasons, with peak values of 10–11 m s^{-1} in January and 11–12 m s^{-1} in July occurring in the Atlantic and Indian Ocean sectors. (These maxima have been rounded down a little in this plot by the smoothing.)

Central pressures

The most notable features of the central pressures of GCM cyclones (Fig. 6) are the zonal symmetry

Fig. 5 Average eastward velocities of cyclones for (a) January and (b) July (contour interval 2 m s^{-1}). (Solid contours indicate eastward and broken lines westward velocities.)

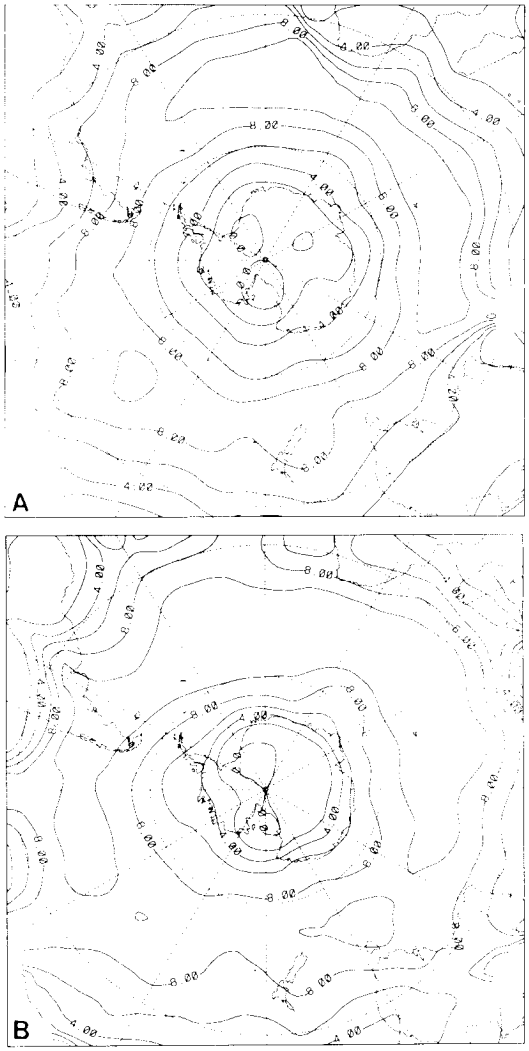

Fig. 6 Average central pressures of cyclones for (a) January and (b) July (contour interval 5 hPa).

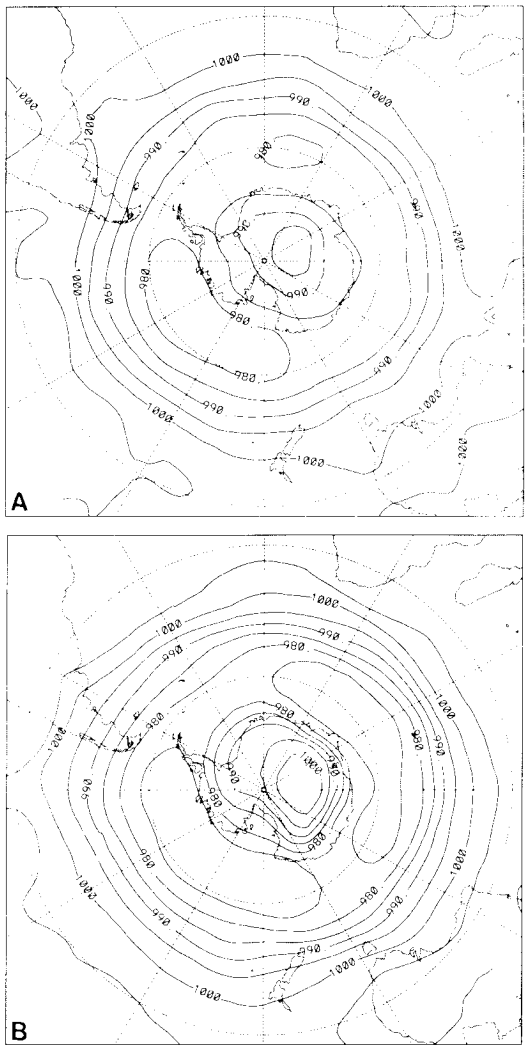

of their distribution and their rapid falling away with latitude between 40° and 50°S. In these respects they are in agreement with those of Karelsky (1963), given for the Australian region only. His charts show that at around latitude 40°S pressures are minimum over the Great Australian Bight in January and maximum over Bass Strait in July: there is some indication of these features in the GCM plots but it is difficult to correlate the smaller scale details of the distributions. Further south the central pressures became higher again, but the levels over East Antarctica are probably unrealistic owing to the great depth over which the extrapolation to mean sea level has taken place.

The variation of average central pressures of cyclones for each month was similar in form to that of the climatological mean (or normal) pressure (*vide* Simmonds et al. 1988) for the respective 600-day periods, but the central pressures were of the order of 15 hPa lower than the normal pressures at most latitudes. Perhaps of more significance than the central pressures are the differences between central normal pressures (Fig. 7). Contrary to what one might expect, it will be observed that areas of maximum difference do not correspond to those of minimum average central pressure (Fig. 6). Minimum differences for both seasons were found in the Ross, Weddell and Lambert basins and in an arc around the coast of

Fig. 7 Normal pressure minus average cyclone central pressures for (a) January and (b) July (contour interval 2.5 hPa).

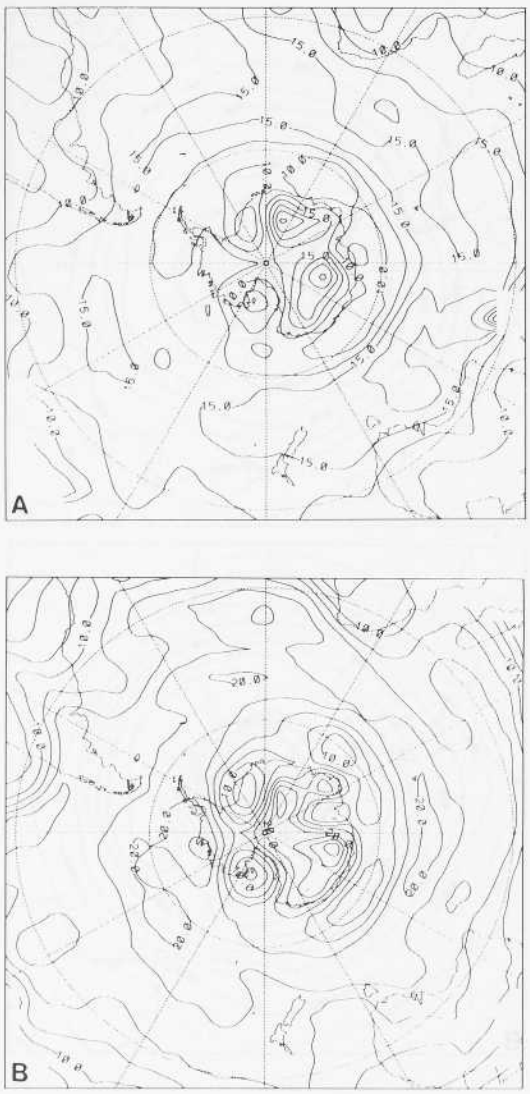

Fig. 8 Positions of cyclogenesis for (a) January and (b) July (cyclones lasting at least four daily positions).

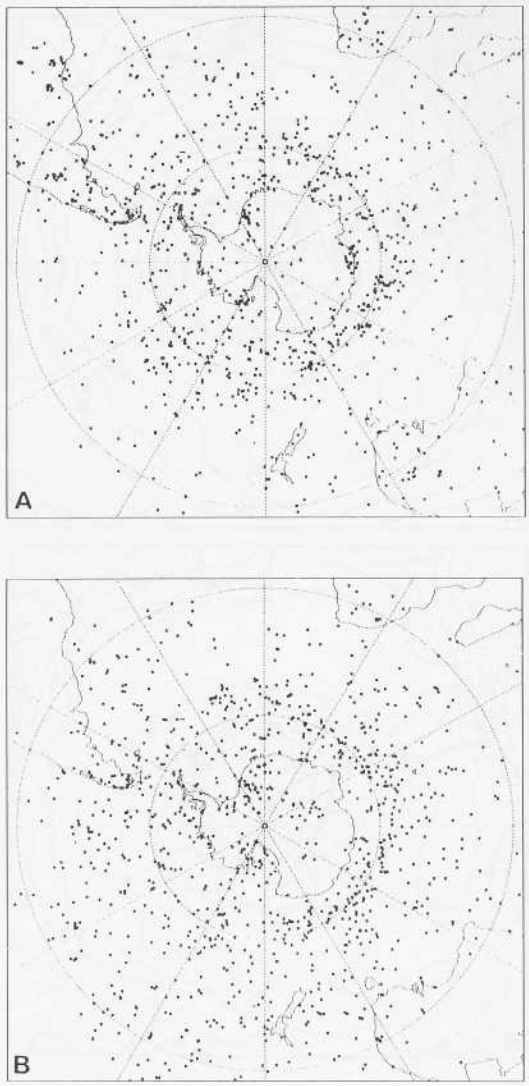

eastern Antarctica. These coincide with the areas of greatest cyclone density shown in Fig. 2. It thus appears that the presence of large numbers of systems over the polar seas contributes to a lowering of average pressures and hence to a diminution of the amplitudes of the pressure variations in these places. It is of interest to note also that there is a good correspondence between the locations of the minima of the pressure difference and those of the standard deviations of the daily MSL pressure analysed from the same GCM data as used here (Simmonds et al. 1990).

Cyclogenesis and cyclolysis

The points of cyclone formation (Fig. 8) may be compared with the points of dissipation (Fig. 9). In order to accentuate their differences, the respective plots have been drawn to include the starting and ending points of only those cyclones recorded on at least four consecutive days. As already mentioned, cyclonic systems have a tendency to drift poleward during their lifetimes and this will be seen to have resulted in a more pronounced clustering of cyclolyses toward high latitudes than in the case of cyclogeneses.

Fig. 9 Positions of cyclolysis for (a) January and (b) July (cyclones lasting at least four daily positions).

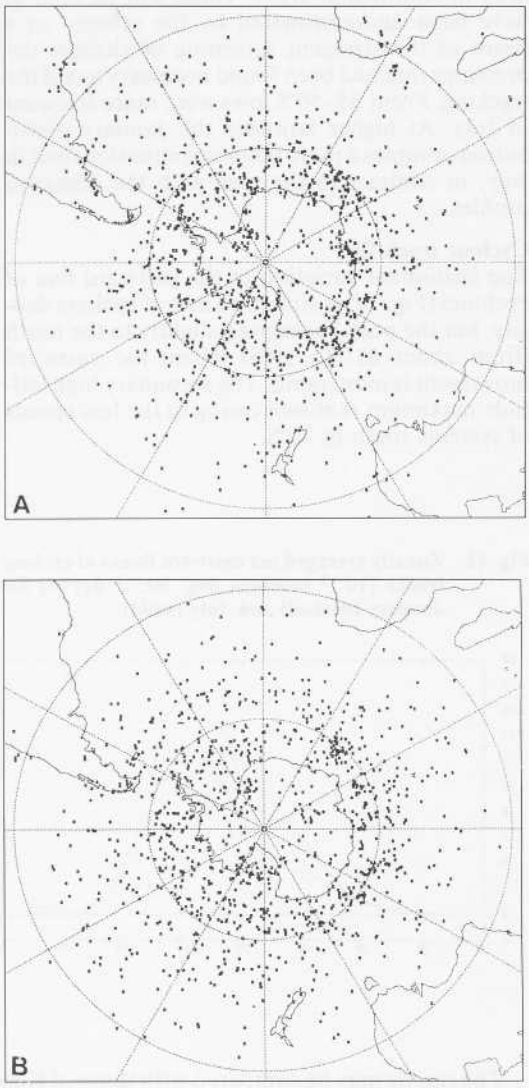

A number of authors (Streten and Troup 1973; Carleton 1979; and Budd 1986) have identified characteristic cyclogenetic and cyclolytic regions, the latter being ascribed particular embayments of the Antarctic coastline. Evidence of such distinctive and localised regions in the plotted positions of Taljaard (1967) and Kep (1984) is tenuous. A comparison of the plotted cyclogeneses of Kep and his corresponding frequency isopleths leads one to believe that a degree of false detail is introduced in contouring areal frequencies from small numbers of events and that too much may have been read into them by some commentators. For this reason the GCM distributions of cyclogenesis and cyclolysis have been presented as plotted positions rather than as frequency isopleths.

It should be noted that the differences between the distributions are only relative, with lows forming and decaying in comparable numbers at all latitudes. Both processes will be seen to peak strongly in the circumpolar trough (in July more so than in January), indicating considerable *in situ* development in this region. This finding is out of keeping with the results of the aforementioned authors who found latitudinal maxima of cyclogenesis near 45°S in both seasons and no appreciable cyclogenesis (in the areas analysed) over Antarctica. This and the close correspondence of the GCM distributions of cyclogenesis and cyclone density would seem to suggest that day-to-day variation in cyclone numbers and tracking errors were exaggerating the incidence of cyclogenesis. On the other hand it may be that the difficulties of detecting new and short-lived systems have led workers in the past to underestimate the level of baroclinic activity at high southern latitudes. Of relevance to this is the study of Mechoso (1980) who has demonstrated the possibility of local cyclogenesis over the Antarctic slopes, caused by a combination of orography, surface drag and strong temperature gradient.

The problem of spurious cyclogenesis can be related to the calculated lifespans of cyclones. For cyclones lasting 24 hours or longer the average lifespan of both January and July cyclones was reckoned to be 4.0 days and 3.7 days, respectively. These durations seem to be in accordance with experience, although we do not have any specific observed estimates with which to compare them. On the other hand, the frequency distribution of cyclone lifespans (Fig. 10) is very skewed, with large numbers of systems being registered at only one or two analysis times and a much smaller number surviving 20 days or longer. We are not yet able to judge how well the GCM results reflect this aspect of the evolution of cyclonic systems in the real atmosphere.

Zonal averages

Cyclone density

The zonally averaged cyclone densities for January and July are shown in Fig. 11. The GCM results may be compared with the meridional profiles of Taljaard (1967) and Le Marshall and Kelly (1981), which have been redrawn as areal densities. One observes a sharply peaked maximum of cyclone occurrence near 60°S in each season, and a subsidiary maximum at about 80°S, corresponding to the lows analysed over the Ross and Weddell Seas. Overall, the distribution south of 45°S for January appears displaced poleward of that for July by a few degrees.

Fig. 10 Frequencies of GCM cyclones by lifespan (difference between times of cyclogenesis and cyclolysis) for July (solid) and January (dashed). Faint lines indicate total numbers of tracks in 600 days and bold traces the integrated lifespan (in days) represented by these tracks.

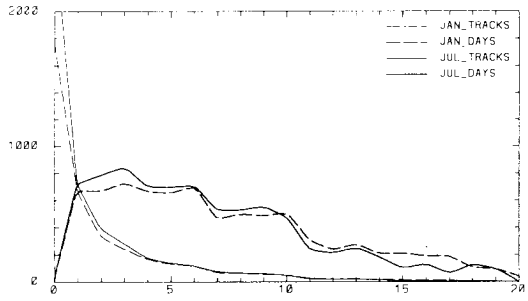

Fig. 11 (a) Zonally averaged cyclone densities (10^{-3} numbers deg. lat.$^{-2}$) for January (dashed) and July (solid). (b) Meridional profiles in the same units from Taljaard (T) and Le Marshall and Kelly (leMK).

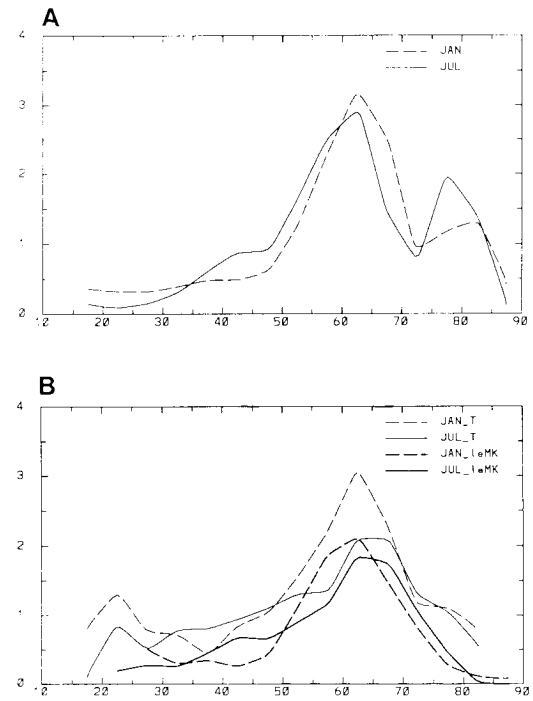

The model results agree with those of these authors in the placement of the circumpolar maximum, but differ in other respects. Both of these observational studies display a more gradual falling away of densities to the north of 60°S and no indication of a secondary peak at high latitudes.

The numbers of cyclones at low latitudes in all three data sets were greater in January than in July, owing principally to the persistence of heat lows in continental areas. These will be seen to have been underestimated by the scheme as a result of the stringent screening of shallow depressions that had been found necessary to aid the tracking. From 35–50°S lows were more frequent in July. At higher latitudes the January distribution occupies a more poleward situation than in July, in contrast to the case with the observed profiles.

Cyclone track flux

The latitudinal variation of the eastward flux of cyclones (Fig. 12) is similar to that of cyclone density, but the peak has moved slightly to the north (from about 61° to 59°S) where the eastward movement is more rapid. The secondary high latitude maximum is absent owing to the low speeds of systems south of 70°S.

Fig. 12 Zonally averaged net eastward fluxes of cyclone tracks (10^{-3} numbers deg. lat.$^{-1}$ day^{-1}) for January (dashed) and July (solid).

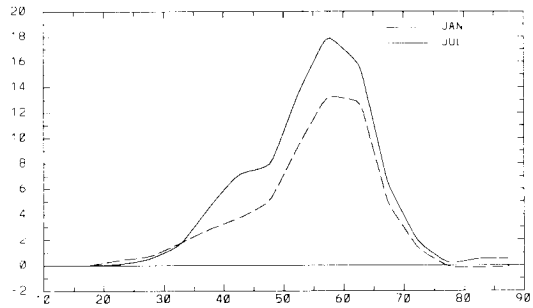

The results may be compared with those of Kep (1984) (reported by Budd (1986)) who obtained maximum numbers of meridian crossings in the eastern sector in the band 50–60°S in both seasons. His peaks are broader than those of the GCM results and particularly so in July (although this was partly a result of using 10° latitude bands).

Velocities

The zonally averaged cyclone velocity components are shown in Fig. 13. It will be seen that the peak eastward velocity occurred in the 45–50°S zone in both seasons but was a little greater in winter, being 11.0 m s^{-1} in July and 10.2 m s^{-1} in January. Average southward movement in each month was 2–4 m s^{-1} in mid-latitudes (25–50°S) falling to 1 m s^{-1} in the circumpolar region.

Fig. 13 Zonally averaged eastward (bold) and northward (lower curves, faint) cyclone velocity components (m s^{-1}) for January (dashed) and July (solid).

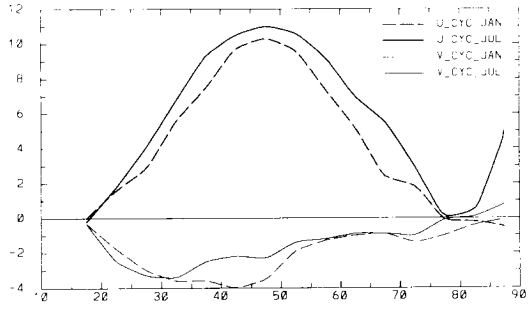

The maximum speed for January, 10.4 m s^{-1} (8.0 deg. lat./day) in the 45–50°S zone, was somewhat lower than the 9.5 deg. lat./day obtained by Streten and Troup (1973) for 40–50°S in summer; also, the speeds of the model cyclones fell away more rapidly at higher latitudes. Streten and Troup did not have observations for winter but their speeds for spring and autumn were slightly greater than in summer, which is in line with our simulations.

Systematic errors in cyclone displacements have been studied by Akyildiz (1985) and also by Grotjahn (1990), using an objective feature-based scheme. The likelihood of similar errors in the GCM results and the dynamical reasons for them warrant further investigation.

Central pressures and tendencies

The zonally averaged central pressure and normal pressure for each season (Fig. 14) varied in a similar fashion, with minima of both functions occurring at the same latitudes. The fall of central pressure with increasing latitude between 45° and 60°S in July was more rapid (1.1 hPa/deg. lat.) and in January less so (0.9 hPa/deg. lat.) than the meridional pressure gradient (1.0 hPa/deg. lat. in both months). The difference between the central and normal pressures (lower curves) might be taken as a measure of the mean relative depth of lows at the latitude: this is seen to have increased from 14 hPa at 40°S to 17 hPa at 60°S in July and to have decreased from 14 hPa to 12 hPa over the same interval in January. This finding would reflect the greater amplitudes of systems in the winter months.

At high latitudes the difference graphs for January and July are similar in form, with the minima in each at around 65° and 80°S corresponding respectively to the regions of low relative depth off East Antarctica and over the West Antarctic basins seen in Fig. 7. The curve for January is about 5 hPa lower and is displaced 5° further south than in July. This displacement may be associated with the contraction of the sea-ice margin in summer.

Fig. 14 (a) Zonally averaged central pressures (hPa) of cyclones (bold) compared with normal pressures from the same simulations (faint) for July (solid) and January (dashed). (b) The difference graphs (normal-central pressure) for the two months are shown in the lower box.

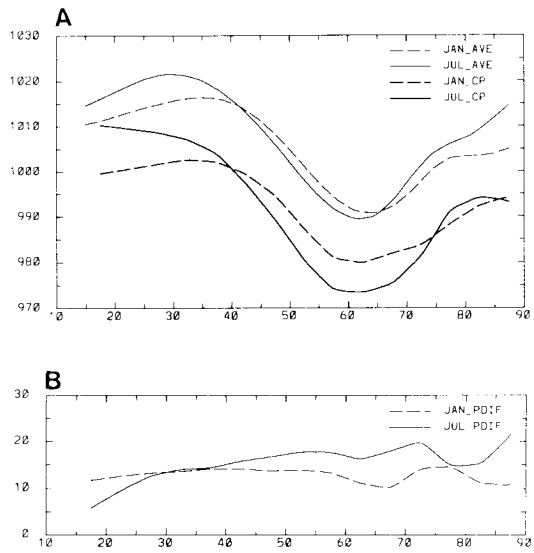

Fig. 15 Zonally averaged central pressure tendencies (hPa/day) of individual cyclones for July (solid) and January (dashed).

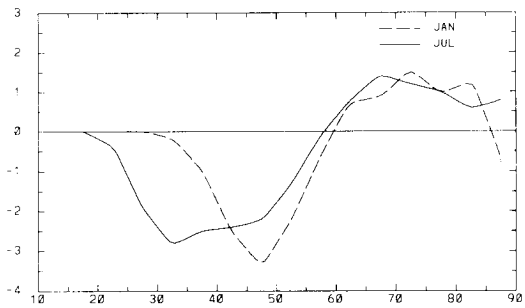

In Fig. 15 we show the zonal average of the central pressure tendency of cyclones as a function of latitude. A mean falling tendency in mid-latitudes of the order of 1–2 hPa/day is in agreement with the overall poleward migration (1–2°/day) of systems and the meridional gradient of central pressure (1 hPa/deg. lat.). The zonally averaged tendencies are, of course, much smaller than the rates of intensification and dissipation of individual storms, which are characteristically in the range 12–20 hPa/day.

Cyclogenesis and cyclolysis

The latitudinal variations of cyclogenesis and cyclolysis are given for cyclones lasting four or more daily positions in Fig. 16. As noted before, the distribution of cyclolysis is biased poleward of that of cyclogenesis, with formation being predominant north of 50°S and dissipation south of 60°S. (The corresponding graphs for cyclones lasting two daily positions were found to demonstrate the same feature, although less strikingly.) Area normalisation of the zonal averages has been omitted in order that total numbers of new and decaying cyclones at different latitudes may be compared.

Fig. 16 Total number of (a) January and (b) July cyclongenesis (faint) and cyclolysis (solid) in 5° latitude zones (for all systems lasting at least four daily positions during the 600-day period).

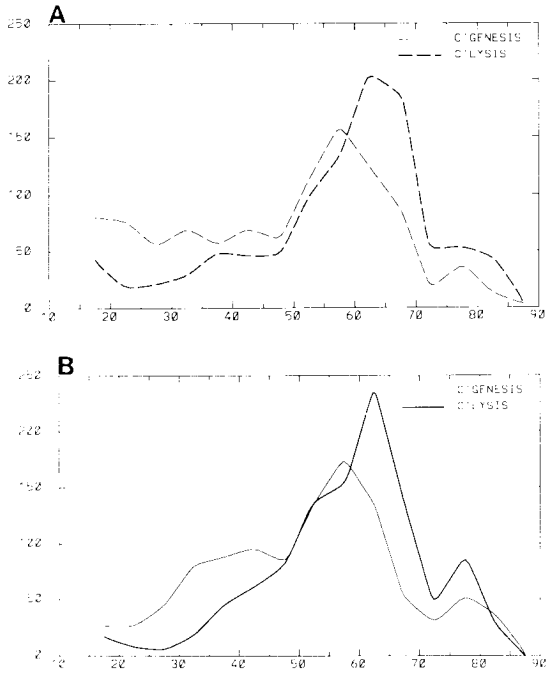

Variability

The movement and distribution of cyclones during any one season may undergo considerable change from year to year (Budd 1982) as shown in the plotted cyclone tracks and zonal cyclogenesis statistics of Kep (1984), and in the meridional profiles of cyclone frequency of Le Marshall and Kelly (1981). An appreciation of the magnitude of this variability and the time-scales over which it is built up are of some importance in constructing any climatology of cyclone behaviour and in establishing secular trends.

In reality, interannual variability in the circulation patterns may be the result of changes in ocean heat storage, sea-ice extent and cloud cover, and of dynamic processes occurring within the atmosphere. In the model climate only the last would be operative and the effects of ocean, ice and cloud would need to be studied with reference to separate modelling experiments.

A measure of the variability in the behaviour of GCM cyclones may be obtained by finding the standard deviation of means taken over a suitably representative sampling period. The standard deviation of 30-day means of a few selected quantities in 10° latitude zones are shown in Table 1, together with the respective 600-day means and the difference between the means for the first and second 300 days.

Discussion and concluding remarks

The behaviour of the GCM cyclones described in this paper appears to be in agreement with most of the features of cyclonic behaviour known from observational studies and synoptic experience. The movement of systems was in a generally east-southeast direction with maximum speeds of 10–11 m s^{-1} (8 deg. lat./day) near 45°S in summer and winter. Cyclone tracks were most concentrated near 60°S in both seasons. Longitudinally, frequencies were greatest in the Indian Ocean sector where cyclone paths tended to be restricted to a narrower range of latitudes. There was a marked tendency for systems to slow down and dissipate close to the Antarctic coast and over the Ross and Weddell Seas. In July the eastward migration of cyclones was more rapid and extended further north than in January.

In some respects the behaviour of the GCM cyclones appeared to be at variance with published climatologies. We have noted (i) a tendency for migratory systems to originate over the continents in summer, (ii) a lower than observed rate of eastward movement in mid to high latitudes, and (iii) a too sharply peaked meridional profile of cyclone density in winter. These discrepancies may be related, at least in part, to the physics of the GCM or the spectral truncation.

The isolation of real differences between observed and model synoptic climatologies is rendered difficult by a number of unavoidable biases encountered in performing this type of investigation. On the one hand the distributions of cyclone frequencies and other properties calculated in this study are sensitive to a variety of factors related to the operation of the scheme. These include unrealistic pressure reductions (over South America and Antarctica), peculiarities of the interpolation, latitude-dependent variations in the grid resolution and background pressure gradients, criteria used in the definition of a low, variation in consecutive daily cyclone

Table 1. Variability statistics (for cyclones lasting 24 hours or longer) showing the 600-day means, the difference between the two 300-day means, and the standard deviations of 30-day means.

Latitude Zone (°S)	*Cyclone density* (10^{-3} *numbers deg. lat.*$^{-2}$) *Ave.*	*Dif.*	*S.D.*	*Eastward velocity* ($m\ s^{-1}$) *Ave.*	*Dif.*	*S.D.*	*Central pressure* (*hPa*) *Ave.*	*Dif.*	*S.D.*
(a) January									
20–30	0.32	0.01	0.08	2.2	0.0	0.8	1001.2	−0.7	1.0
30–40	0.43	0.00	0.11	6.6	0.8	1.0	1002.3	0.5	1.2
40–50	0.55	−0.02	0.14	10.0	0.4	0.9	996.8	1.3	2.0
50–60	1.74	0.05	0.44	8.2	0.4	0.8	983.4	0.1	1.2
60–70	2.86	−0.05	0.48	4.1	−0.1	0.7	980.7	0.4	2.3
70–80	1.05	0.22	0.28	0.9	0.3	1.4	986.0	1.8	4.9
80–90	1.08	0.05	0.28	−0.2	0.4	1.3	992.5	1.1	5.9
(b) July									
20–30	0.12	−0.03	0.05	3.2	0.1	1.9	1008.9	0.3	2.3
30–40	0.46	0.01	0.11	8.4	0.2	1.1	1004.9	0.4	2.1
40–50	0.90	−0.04	0.23	10.8	0.5	1.1	993.3	0.1	1.9
50–60	2.04	0.01	0.38	9.8	0.0	0.6	976.8	−1.1	1.7
60–70	2.25	0.02	0.36	6.6	0.3	0.6	974.0	0.1	1.9
70–80	1.29	0.07	0.25	1.1	−0.4	1.3	987.7	1.1	4.3
80–90	1.08	0.06	0.34	0.6	0.5	1.4	994.1	−1.0	4.9

numbers, and tracking errors. A number of these factors also apply to observational studies where there may be problems with data coverage and quality. From theoretical and recent observational studies it appears likely that the sparsity of data at high southern latitudes may have resulted in an underestimation of cyclonic activity in this region by earlier authors, and that the occurrence of GCM cyclones over the Ross and Weddell Seas and parts of the Antarctic continent and the high frequency of local cyclogenesis in the circumpolar trough may be realistic and not just an artifact of the tracking scheme.

Owing to the inherent limitations of manual techniques, the statistics available from earlier work are mostly limited to frequencies of cyclone occurrence and cyclogenesis. In most of these studies, the delineation of preferred tracks has been inferred from ridges in cyclone frequency isopleths rather than from the actual alignment of depression paths. Very little has been documented concerning average velocities, central pressures and lifespans. Unfortunately the absence of digitised track histories rules out the possibility of reworking the data to obtain these and other statistics. These remarks underline the need to conduct a similar objective analysis of cyclone behaviour from real numerical data to help us fill these gaps in our knowledge.

From the foregoing considerations we suggest that the behaviour of the extratropical cyclones embodied in the GCM data is realistic and that the scheme may be applied with confidence to a number of climate simulations. The possibility of biases, such as we have drawn attention to, would not be a deterrent to its application to comparative studies.

An important application of the scheme will be its use in GCM sensitivity studies, and specifically those germane to expected future climate changes. Data from these experiments have mainly been used for studying changes in the mean states of the atmospheric variables, but the features of most interest may be the changes induced in synoptic behaviour and the implication these will have for climate. An example of the type of application we have in mind would be an elucidation of the role of thermal contrasts and surface fluxes in the sea-ice zone in accounting for the concentration and latitudinal variability of cyclonic activity in the polar oceans. Other examples would include the synoptic changes induced by changes in sea-surface temperatures and carbon dioxide.

References

Akyildiz, V., 1985. Systematic errors in the behaviour of cyclones in the ECMWF operational model. *Tellus, 37A*, 297–308.

Budd, W.F., 1982. The role of Antarctica in southern hemisphere weather and climate. *Aust. Met. Mag., 30*, 265–72.

Budd, W.F., 1986. The Southern Hemisphere circulation of atmosphere ocean and sea ice. *Proceedings of the Second International Conference on Southern Hemisphere Meteorology, December 1986*, Wellington, New Zealand. Amer. Met. Soc., 101–6.

Carleton, A.M., 1979. A Synoptic Climatology of Satellite-Observed Extratropical Cyclone Activity for the Southern Hemisphere Winter. *Arch. Met. Geophys. Bioklim., B, 27*, 265–79.

Grotjahn, R., 1990. Feature-Based Predictability of 500 hpa Height in the Australia-New Zealand Region. *Meteorol. Atmos. Phys., 42*, 57–67.

James, I.N. and Anderson, D.L.T. 1984. Seasonal mean flow and distribution of large-scale weather systems in the Southern Hemisphere: the effects of moisture transports. *Q. Jl R. met. Soc., 110*, 943–66.

Karelsky, S. 1961. Monthly and Seasonal Anticyclonicity and Cyclonicity in the Australian Region — 15 years (1946–1960) Averages. *Met. Study No. 13*, AGPS, Canberra.

Karelsky, S. 1963. Geographical Distribution of Pressure in the Centres of Surface Lows and Highs in the Australian Region in January and July, 1952–1963. *Aust. Met. Mag., 43*, 15–23.

Kep, S.I., 1984. A Climatology of Cyclogenesis, Cyclone Tracks and Cyclolysis in the Southern Hemisphere for the period 1972–81. *Publication No. 25*, Department of Meteorology, University of Melbourne.

Klein, W.H. 1957. Principal tracks and mean frequencies of cyclones and anticyclones in the Northern Hemisphere. *Res. Pap. No. 40*, U.S. Weather Bureau, Washington D.C., 60 pp.

Lambert, S.J. 1988. A Cyclone Climatology of the Canadian Climate Centre General Circulation Model. *J. Climate, 1*, 109–15.

Leighton, R.M. and Deslandes, R. 1989. Monthly Averages of Anticyclonicity and Cyclonicity in the Australasian Region. *Third International Conference on Southern Hemisphere Meteorology and Oceanography, November 1989*, Buenos Aires, Amer. Met. Soc., 245–8.

Le Marshall, J.F. and Kelly, G.A.M. 1981. A January and July climatology of the Southern Hemisphere based on daily numerical analyses 1973–77. *Aust. Met. Mag., 29*, 115–23.

Le Treut, H. and Kalnay, E. 1990. Comparison of observed and simulated cyclone frequency distribution as determined by an objective method. *Atmosfera, 3*, 57–71.

Mechoso, C.R. 1980. The atmospheric circulation around Antarctica: Linear stability and finite amplitude interactions with migrating cyclones. *J. Atmos. Sci., 37*, 2209–33.

Murray, R.J. and Simmonds, I. 1991. A numerical scheme for tracking cyclone centres from digital data. Part I: development and operation of the scheme. *Aust. Met. Mag., 39*, 155–66.

Neal, A.B. 1972. MSL Cyclones and Anticyclones in November 1969 and June 1970. *Aust. Met. Mag., 20*, 217–30.

Oort, A.H. and Peixoto, J.P. 1983. Global angular momentum and energy balance requirements from observations. *Adv. Geophys., 25*, 355–490.

Simmonds, I. 1985. Analysis of the 'spinup' of a general circulation model. *J. Geophys. Res., 90*, 5637–60.

Simmonds, I., Trigg, G. and Law, R. 1988. The Climatology of the Melbourne University General Circulation Model. *Publication No. 31*, Department of Meteorology, University of Melbourne, 67pp.

Simmonds, I. and Dix, M. 1989. The use of mean atmospheric parameters in the calculation of modeled mean surface heat fluxes over the world's oceans. *J. Phys. Oceanogr., 19*, 205–15.

Simmonds, I., Indusekharan, P. and Murray R.J. 1990. A comparison of modelled and observed daily variability in the southern extratropics. *Aust. Met. Mag., 38*, 261–70.

Streten, N.A. 1973. Some Characteristics of Satellite-Observed Bands of Persistent Cloudiness Over the Southern Hemisphere. *Mon. Weath. Rev., 101*, 486–95.

Streten, N.A. and Troup, A.J. 1973. A synoptic climatology of satellite observed cloud vortices over the Southern Hemisphere. *Q. Jl R. met. Soc., 99*, 56–72.

Taljaard, J.J. 1967. Development, Distribution, and Movement of Cyclones and Anticyclones in the Southern Hemisphere during the IGY. *Jnl appl. Met., 6*, 973–87.

Troup, A.J. and Streten, N.A. 1972. Satellite-Observed Southern Hemisphere Cloud Vortices in Relation to Conventional Observations. *Jnl appl. Met., 11*, 909–17.

van Loon, H. 1965. A Climatological Study of the Atmospheric Circulation in the Southern Hemisphere during the IGY, Part I: 1 July 1957–31 March 1958. *Jnl appl. Met., 4*, 479–91.

Whittaker, L.M. and Horn, L.H. 1982. *Atlas of Northern Hemisphere Extratropical Cyclone Activity, 1958–1977*, University of Wisconsin, 65 pp.

Yasunari, T. 1977. Stationary Waves in the Southern Hemisphere Midlatitude Zone Revealed from Average Brightness Charts. *J. met. Soc. Japan, 55*, 274–85.